Journal of Applied Sciences

ISSN 1812-5654

science alert

ANSInet
an open access publisher
http://ansinet.com

Journal of Applied Sciences 8 (9): 1632-1641, 2008
ISSN 1812-5654

Proportional Mixing of Microfluidic Flows Utilizing DC and AC Electric Fields in a T-type Microchannel

[1]W.J. Luo, [2]K.C. Chang and [3]J.S. Wang
[1]Department of Refrigeration, Air-Conditioning and Energy Engineering,
National Chin-Yi University of Technology, Taiping City, Taichung County 411, Taiwan
[2]Department of Electronic Engineering, Far East University, Tainan, Taiwan
[3]Department of Power Mechanical Engineering, National Taitung College, Taitung, Taiwan

Abstract: This research demonstrates the mixing of two-dimensional, time-dependent elestro-osmotic flows in a T-shaped microchannel via the application of a rectified AC electric field at one inlet channel and a DC electric field at the other. By specifying appropriate electric field intensities at the two inlets, a momentum imbalance is induced at the interface between the two fluid streams. This imbalance prompts the formation of a periodic waveform at the interface, which propagates in the downstream direction, resulting in an enhanced mixing of the two species. The characteristics of the micromixer are investigated by performing a series of numerical simulations using the backwards-Euler time-stepping scheme. The results show that the relative proportion of the two fluid streams entering the mixing channel can be adjusted by regulating the difference in intensity of the two electric fields. For a given AC electric field, two threshold values of the DC electric field intensity are found, corresponding to fully-mixed dimensionless concentrations of zero (upper inlet fluid only) and one (lower inlet fluid only), respectively. The dimensionless concentration obtained at DC intensities between these two threshold values varies linearly with the difference in intensity of the two electric fields, but is independent of the frequency of the AC electric field. Finally, varying the width of the mixing channel has no significant effect on the mixing performance (provided that the mixing length is adequately extended) and results in no more than a minor expansion of the linear range bounded by the two DC voltage threshold values.

Key words: Elestro-osmosis, electrical fields, mixing efficiency

INTRODUCTION

Microfluidic devices have found widespread application in clinical practice and throughout the food and chemical industries. The micro-scale flow channels incorporated in such devices increase the surface-to-volume ratio of the fluid streams and are therefore advantageous in many applications, including DNA restriction, multiple sample injection, sample extraction, controlled fraction mixing and so forth. However, the fluid flow within the microchannel is constrained to very low Reynolds numbers (typically <10) and thus homogenization of the species solutions takes place through diffusion processes alone. Consequently, obtaining a satisfactory mixing performance requires the use of extended mixing channels and longer mixing times, which diminish the practical benefits of such devices.

The diffusion of two sample streams can be improved by increasing the interfacial contact area between them. Previous researchers have proposed various passive microfluidic devices which exploit this phenomenon to create an enhanced mixing effect. Feeding the different samples through discrete via holes (Miyake *et al*., 1993), utilizing cantilever plate valves (Voldman *et al*., 2000), configuring the device with multiple channels (Yang *et al*., 2005) and so forth. The feasibility of achieving species mixing via an alternate stretching and folding of the sample flows has also been demonstrated. Branerbjerg *et al*. (1996) reported an effective mixing performance within mixing lengths as short as 100-300 ms. Mengeaud *et al*. (2002) presented a series of Y-form micromixers with various zigzag mixing channel configurations. Luo *et al*. (2005) and Chen *et al*. (2006) investigated the elestro-osmotic flow driven by DC or AC electric fields in a curved microchannel. It is found some circulations induced in the secondary flows can be used to enhance the microfluidic mixing efficiency. Passive micromixers utilizing surface hetereogeneities to

Corresponding Author: Win-Jet Luo, Department of Refrigeration, Air-Conditioning and Energy Engineering, National Chin-Yi University of Technology, Taiping City, Taichung County 411, Taiwan
Tel: 886-6-23924505/8255 Fax: 886-6-23932758

stir the mixing species have also been demonstrated. For example, Ajdari (1995) investigated the complex elestro-osmotic flows induced by the application of non-uniform, time-independent and time-dependent potentials along the conduit walls. Similarly, Qian and Bau (2002) performed a theoretical investigation into two-dimensional, time-independent and time-dependent elestro-osmotic flows driven by a uniform electric field in a conduit with a non-uniform potential distribution. The results showed that time-wise periodic alternations of the potentials induced a chaotic advection effect within the fluid. Erickson and Li (2002) performed three-dimensional numerical simulations to study the effects of surface electrokinetic heterogeneities on the elestro-osmotic flow induced by a uniform electric field and then exploited these effects to enhance the mixing efficiency of a T-shaped micromixer. Biddiss *et al.* (2004) employed an experimental visualization technique to investigate the effects of surface charge patterning on species mixing and presented an optimized electrokinetic micromixer applicable to species mixing in the low Reynolds number regime. Chang and Yang (2004) used a numerical method to simulate the mixing mechanisms of elestro-osmotic flow induced by a DC electric field in a microchannel with oppositely charged surface heterogeneities. The results showed that local flow circulation regions promoted species mixing in the microchannel. Luo (2006) and Luo *et al.* (2007a) demonstrated the mixing of two-dimensional, time-dependent elestro-osmotic flows via the application of an AC electric field to a microchannel patterned with surface heterogeneities. The results showed that the interaction of the AC electric field with the patchwise surface heterogeneities created vortex structures within the fluid streams, which yielded a significant reduction in both the mixing channel length and the retention time required to attain a homogeneous solution. Luo *et al.* (2008) utilized electrical field intensity perturbations to stir the electrokinetic instability in order to enhance the microfluidic mixing in a T-type microchannel. Compared to the passive and active schemes presented in the literature, such EKI-based schemes have the advantages of a simpler microchannel design, a more straightforward fabrication process and a rudimentary voltage control scheme.

In addition to the passive mixing schemes, described above, researchers have also proposed many active mixing schemes, in which species mixing is achieved via the application of an external force to the fluid flow. For example, Rife *et al.* (2000) demonstrated the use of embedded PZT ultrasonic transducers to generate acoustic waves to stir the samples within the mixing channel. Meanwhile, Lu *et al.* (2002) proposed a sophisticated micromixer incorporating micro-magnetic stirrers fabricated using surface micromachining techniques. Lee *et al.* (2001) developed a microfluidic device featuring embedded microelectrodes to induce the dielectrophoretic stretching and folding of sample fluids. Oddy *et al.* (2001) demonstrated the feasibility of using electrokinetic instability effects to achieve the rapid mixing of micro- and nano-liter volume solutions for bioanalytical applications. Luo *et al.* (2007b) presented a T-form micromixer which utilized a rectified AC electric field and a DC electric field to induced elestro-osmotic flows for sample proportional mixing.

Electrokinetic flow has emerged as the method of choice for transporting species in microfluidic devices designed to carry out immunoassays, DNA hybridization and general cell-molecule interaction applications. In general, such applications require the rapid and efficient mixing of two or more species. Accordingly, the present study proposes a T-shaped micromixer in which an enhanced mixing performance is obtained by applying AC and DC electric fields at the upper and lower inlets, respectively, while grounding the outlet. The characteristics of the proposed micromixer are investigated by performing a series of simulations based upon the backwards-Euler time-stepping method. The simulations focus specifically on the respective effects on the mixing performance of the difference in intensity of the AC and DC electric fields, the frequency of the AC electric field and the width of the mixing channel. In general, the results confirm the feasibility of the proposed approach in accomplishing the proportional mixing of microfluidic flows within a finite time and mixing distance.

FORMULATION

The T-shaped microchannel considered in the present study (Fig. 1) has a nominal width and height of 60 mm and is filled with an incompressible Newtonian electrolyte of uniform dielectric constant, ε and viscosity, μ. Since the characteristic height of the microchannel is in the order of magnitude of 10 mm, the interaction between the fluid and the walls is significant and must be taken into account in the theoretical model. A review of the literature suggests that a theoretical model comprising the Poisson-Boltzmann equation, the Laplace equation and the Navier-Stokes equation with body force terms from the Guoy-Chapman model provides a reasonable description of the elestro-osmotic flow in the current microchannel. Furthermore, the distributions of the electrical double layer potential and the applied electric field can be described using the Poisson-Boltzmann equation and the Laplace equation, respectively.

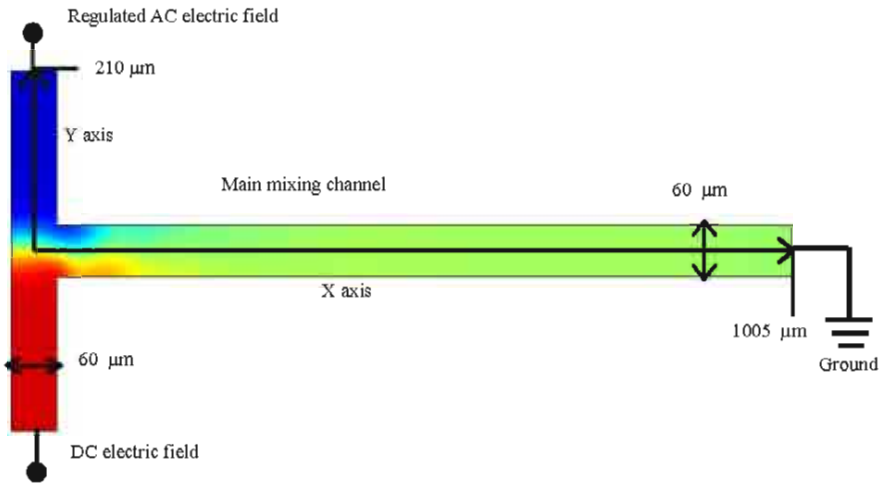

Fig. 1: Schematic illustration of T-shaped microchannel showing principal dimensions and fluid flows

Distributions of electric field and electrical double layer potential: The non-dimensional quantities (denoted by an asterisk) are defined as following:

$$x^* = \frac{x}{A}, \quad y^* = \frac{y}{A}, \quad \psi^* = \frac{ze\psi}{k_b T}, \quad \phi^* = \frac{ze\phi}{k_b T}$$

The distribution of the applied electric field is governed by the Laplace equation, i.e.,

$$\frac{\partial^2 \phi}{\partial x^2} + \frac{\partial^2 \phi}{\partial y^2} = 0 \tag{1}$$

According to electrostatics theory, the distribution of the electric potential in the EDL is governed by the Poisson-Boltzmann equation (Hunter, 1986). The dimensionless non-linear Poisson-Boltzmann distribution equation can then be expressed as:

$$\frac{\partial^2 \psi}{\partial x^2} + \frac{\partial^2 \psi}{\partial y^2} = \kappa^2 \sinh(\psi) \tag{2}$$

where, ψ is the non-dimensional EDL potential, $\kappa = A \times K$ is the non-dimensional EDL thickness, $K = (2n_0 z_z e_2/\varepsilon\varepsilon_0 k_b T)^{1/2}$ is the Debye-Huckel parameter, where ε is the dielectric constant of the fluid, z is the valence, e is the charge carried by an electron, n_o is the bulk electrolyte concentration, k_b is the Boltzmann constant and T is the temperature and A is the height of the microchannel (Note that the asterisks are omitted here for convenience) (Table 1).

Electro-osmotic flow field: When an external electric field is applied to the microchannel, the resulting liquid flow induced by elestro-osmosis is governed by the momentum equation (Dutta and Beskok, 2001; Yang and Li, 1998), i.e.,

Table 1: Parameters employed in numerical analysis

Microchannel height A (μm)	60
Fluid viscosity μ (N s m^{-2})	0.90×10^{-3}
Fluid density ρ (kg m^{-3})	10^3
Ionic concentration ξ (m)	10^{-6}
Dielectric constant ε	78.3
Permittivity of vacuum ε_0 (F m^{-1})	8.854×10^{-12}
Electron charge e (c)	1.6021×10^{-19}
Valence Z	1
Bulk electrolyte concentration (n_b m^{-3})	6.022×10^{20}
Boltzmann constant k_b (J K^{-1})	1.38×10^{-23}
Absolute temperature T (K)	298.16
Electrical double layer potential ψ (mV)	-75

$$\rho\frac{\partial V}{\partial t} + \rho(V \cdot \nabla)V = -\nabla P + F + \mu\nabla^2 V \tag{3}$$

Assuming that the gravity effect is very small and can be neglected, the only force (F) acting on the fluid is that produced by the interaction between the applied electric field and the free ions within the EDL. This body force induces a bulk fluid motion generally referred to as elestro-osmotic flow. The following non-dimensional quantities (denoted by asterisks) can be introduced: non-dimensional velocity $u^* = u/(\upsilon/A)$ or $v^* = v/(\upsilon/A)$, non-dimensional time $t^* = t/(A^2/\upsilon)$, non-dimensional pressure $p^* = (p-p_{ref})/(\rho\upsilon^2/A^2)$ and non-dimensional angular velocity $\Lambda^* = \Lambda/(\upsilon/A^2)$, where υ is the kinetic viscosity of the electrolyte, t is time and Λ is the angular velocity of the applied electric field, i.e., $\Lambda = 2\pi f$. Hence, the momentum equation given in Eq. 3 can be rewritten as:

$$\frac{\partial u}{\partial x} + \frac{\partial v}{\partial y} = 0 \tag{4a}$$

$$\frac{\partial u}{\partial t}+u\frac{\partial u}{\partial x}+v\frac{\partial u}{\partial y}+\frac{\partial p}{\partial x}-\frac{\partial^2 u}{\partial x^2}-\frac{\partial^2 u}{\partial y^2}-G_x\cdot\sinh\psi\left(\frac{\partial\psi}{\partial x}+\frac{\partial\phi}{\partial x}\right)=0 \quad (4b)$$

$$\frac{\partial v}{\partial t}+u\frac{\partial v}{\partial x}+v\frac{\partial v}{\partial y}+\frac{\partial p}{\partial y}-\frac{\partial^2 v}{\partial x^2}-\frac{\partial^2 v}{\partial y^2}-G_x\cdot\sinh\psi\left(\frac{\partial\psi}{\partial y}+\frac{\partial\phi}{\partial y}\right)=0 \quad (4c)$$

where, $Gx = 2n_0k_bT/(\rho V^2/A^2)$ and ϕ is the applied electric potential. The Reynolds number is defined as uA/υ. Hence, according to the definition of the non-dimensional velocity quantity, the Reynolds number in the current T-shaped microchannel has a value of one, as indicated by Eq. 4b and c.

Concentration field: The species mixing of elestro-osmotic flows can be described by the following dimensionless concentration equation:

$$\frac{\partial C}{\partial t}+u\frac{\partial C}{\partial x}+v\frac{\partial C}{\partial y}=\frac{1}{Pe}\left(\frac{\partial^2 C}{\partial x^2}+\frac{\partial^2 C}{\partial y^2}\right) \quad (5)$$

where, C is the non-dimensional concentration of the species and $Pe = U_{ref}A/D_i$, where D_i is the diffusion coefficient of the species. The mixing efficiency at any point in the mixing channel can be evaluated by:

$$\sigma(x)=\left(1-\frac{\int_0^A (C-C_{ref})dy}{\int_0^A (C_0-C_{ref})dy}\right)\times 100\% \quad (6)$$

where, C is the non-dimensional species concentration profile across the width of the mixing channel and C_0 and C_{ref} are the solution concentrations in the completely unmixed and completely mixed states, respectively.

Boundary conditions: In the current simulations, the microchannel surfaces are assumed to be homogeneous and to have a zeta potential of -75 mV, equivalent to a dimensionless value of $\psi = 2.92$. The boundary conditions at the walls, inlets and outlet of the microchannel are given as follows:

- At the walls, with no-slip conditions:

  $u = 0,\ v = 0$

  $$\frac{\partial p}{\partial n}=\frac{\partial^2 u}{Re\,\partial n^2}+G_x\cdot\sinh\psi\frac{\partial\psi}{\partial n} \quad \text{or}$$

  $$\frac{\partial p}{\partial n}=\frac{\partial^2 v}{Re\,\partial n^2}+G_x\cdot\sinh\psi\frac{\partial\psi}{\partial n},$$

  $$\frac{\partial C}{\partial n}=0,\quad \frac{\partial\phi}{\partial n}=0,$$

  $$\psi=-2.92$$

  Note that n denotes the normal unit vector to the microchannel walls.

- At the inlets:
  $\partial\psi/\partial y = 0$, $\phi = \phi_m|\sin \Lambda t|$ at the upper inlet, ϕ = Const. at the lower inlet.
  $u = 0$, $\partial\psi/\partial y = 0$, $p = 0$, $C = 0$ at the upper inlet, $C = 1$ at the lower inlet.

  Note that ϕ_m denotes the maximum electric potential generated by the AC electric power supply.
- At the outlet:

  $$\frac{\partial\psi}{\partial x}=0,\ \phi=0,$$

  $$\frac{\partial u}{\partial x}=0,\ \frac{\partial v}{\partial x}=0,\ p=0,\ \frac{\partial C}{\partial x}=0$$

Full details of the physical models about the elestro-osmotic flow are reported in Luo *et al.* (2006, 2007) and Luo (2006).

Numerical method: The numerical solution procedure performed in this study employs the backwards-Euler time-stepping method to identify the evolution of the flow when driven by the AC electric field. The applied electric potential, ϕ, can be computed from the Laplace equation given in Eq. 1, while the zeta potential distribution in the EDL can be obtained from Eq. 2. The transient elestro-osmotic flow under the applied electric field can then be simulated by substituting the electric potential into Eq. 4b and c and solving the simplified equation set given in Eq. 4a-c. The computational domain is discretized into 351×701 non-equally spaced grid points in the X- and Y-directions. The calculated solutions were proven to be independent of both the computational grid points and the time step. Full details of the iteration algorithm about the backwards-Euler time-stepping method are reported in Yang and Luo (2002) and Luo (2004a, b).

RESULTS AND DISCUSSION

As shown in Fig. 1, this study considers a T-shaped microchannel in which electrodes are installed at the two inlets and the outlet is connected to ground. During the mixing operation, a DC electric field is applied to the lower inlet, while an AC electric field is applied to the upper inlet. The intensity of the DC electric field is assigned a sufficiently high value to ensure that the fluid entering the microchannel through the lower inlet has sufficient momentum to drive the fluid stream entering through the upper inlet into the mixing channel. Furthermore, half-wave rectification is applied to the AC electric field at the upper inlet to prevent the injected fluid from returning to the reservoir. In practice, the relative proportion of the two fluid streams entering the mixing channel (and hence the final solution concentration obtained in the fully-

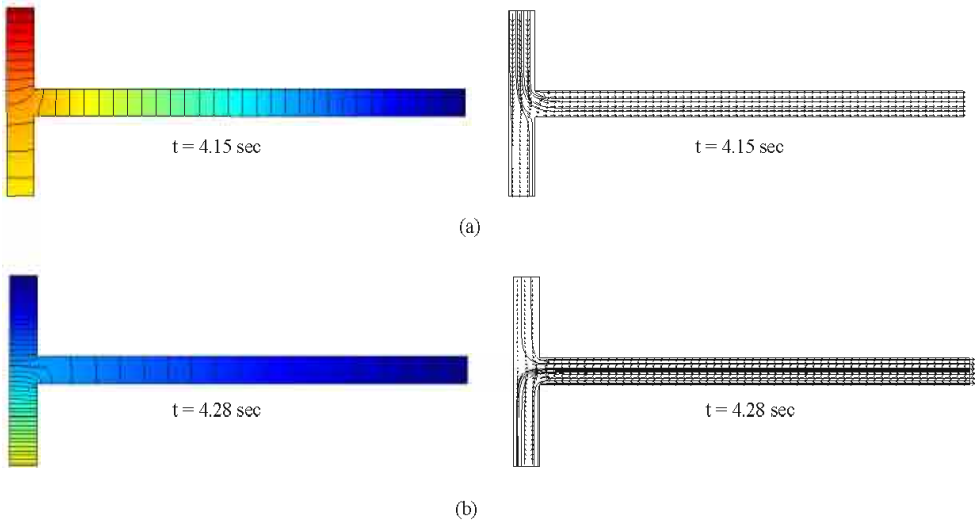

Fig. 2: Evolutions of electric field and flow field, respectively, under application of AC electric field of intensity 165 V/cm and frequency 4 Hz at upper inlet and constant DC electric field intensity of 105 V/cm at lower inlet

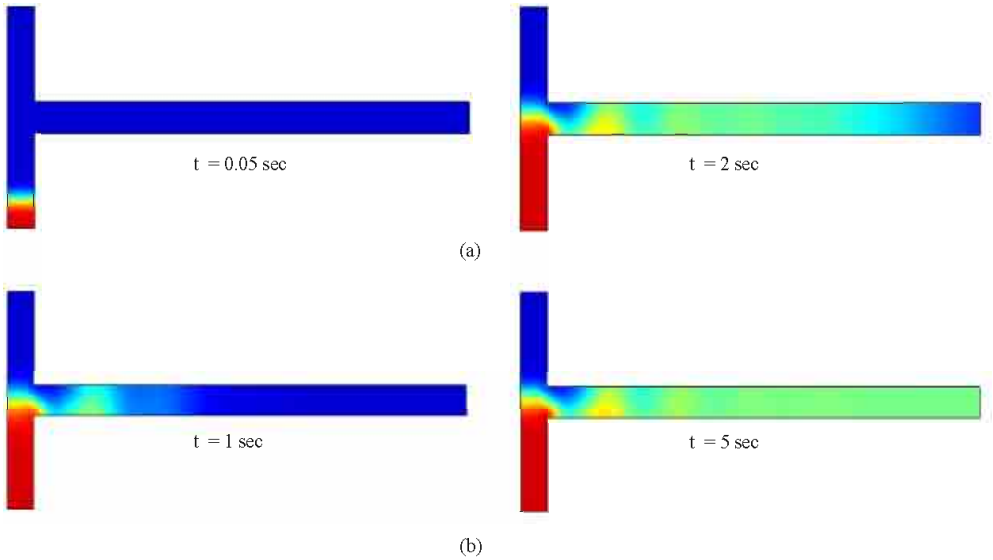

Fig. 3: Evolution of concentration under application of AC electric field of amplitude 165 V/cm and frequency 4 Hz applied at upper inlet and constant DC electric field intensity of 105 V/cm applied at lower inlet

mixed state) is easily controlled by maintaining a constant AC electric field intensity at the upper inlet while regulating the value of the DC electric field intensity applied at the lower inlet.

As shown in Fig. 2a, when the amplitude of the AC electric field intensity is greater than that of the DC electric field, most of the fluid in the main mixing channel originates from the upper inlet. Conversely, when the amplitude of the AC electric field intensity is less than that of the DC electric field, the fluid in the mixing channel originates primarily from the lower inlet, as shown in Fig. 2b and c. Overall, the results presented in Fig. 2 indicate that the relative proportion of the two flow streams entering the mixing channel is governed by the relative intensities of the AC and DC electric fields.

Figure 3 presents the temporal evolution of the concentration field within the microchannel over the course of a single period of the AC electric field. Note that the AC electric field has an amplitude of 165 V/cm and a frequency of 4 Hz, while the DC electric field has an

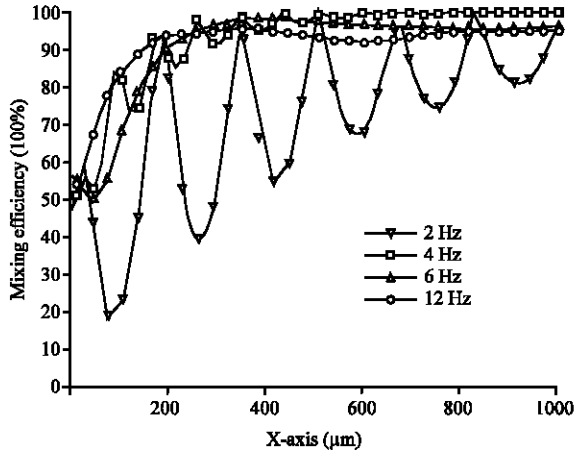

Fig. 4: Variation of mixing efficiency along main channel under application of AC electric field of amplitude 165 V/cm and frequency 2, 4, 6, 12 Hz at upper inlet and constant DC electric field intensity of 105 V/cm at lower inlet when t = 5 sec

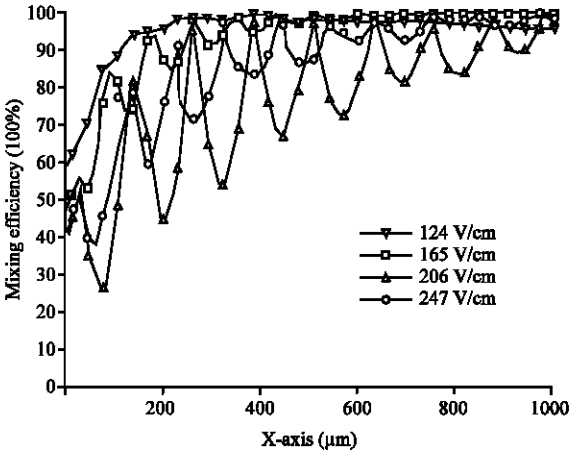

Fig. 5: Variation of mixing efficiency along main channel under application of AC electric field of amplitude 124, 165, 206, 247 V/cm and frequency 4 Hz at upper inlet and constant DC electric field intensity of 105 V/cm at lower inlet when t = 4.6 sec

amplitude of 105 V/cm. As shown, the applied electric fields cause the two species with different concentrations (i.e., zero in the upper inlet and one in the lower inlet) to converge in the junction region of the microchannel. Due to the difference in intensity of the AC and DC electric fields, a momentum imbalance arises at the interface of the two fluid flows, resulting in the formation of a periodic waveform, which propagates in the downstream direction at the velocity of the elestro-osmotic flow. The wave-like interface increases the contact area of the two species and therefore enhances the convective mixing effect between them. Figure 4 shows the corresponding variations of the mixing efficiency along the length of the main mixing channel with different frequency of the applied AC electric field. At low frequency (2 Hz), the amount of the samples to be injected into the mixing channel during a period is greater than those at high frequency and the injected samples from a series of patches staggered along the main mixing channel. Therefore, the distribution of the corresponding mixing efficiency along the mixing channel appears with high amplitude. At high frequency (6 and 12 Hz), the samples can be effectively mixed at the entrance of the mixing channel through the induced high frequency waveform flow. However, the amplitudes of these induced high frequency waveform flows are much smaller and these high frequency waveform flows can not be propagated far in the downstream. Therefore, the effective mixing efficiency can not be sustained in the downstream of the mixing channel. From inspection, it is found that for the case with frequency of 4 Hz, a mixing efficiency as high as 92% can be achieved within a mixing distance of 0.6 mm. The performance of the 4 Hz case is the best among the cases. For the case with high amplitude of the applied AC electric field intensity (206 and 247 V/cm), the amplitude of the induced waveform flow is also greater and the distribution of the corresponding mixing efficiency also appears with a wavy form with greater amplitude (Fig. 5). For the case with low amplitude of the applied AC electric field intensity (124 V/cm), the amplitude of the induced waveform flow becomes smaller. The induced waveform flows can not be propagated far in the downstream and the effective mixing efficiency can not be sustained in the downstream of the mixing channel. In the Fig. 5, it can be found the mixing performance of the case with the amplitude of 165 V/cm is the best among the cases. For the case with the application of the AC electric field with the amplitude of 165 V/cm and the frequency of 4 Hz, a mixing efficiency as high as 90% can be achieved at t = 2.6 sec and the fully-mixed cab be achieved at t = 4.6 sec. However, for the case with the application of the AC electric field with the amplitude of 124 V/cm and the frequency of 4 Hz, the driving electric force is smaller (Fig. 6). A time of 3.65 sec is required to achieve a mixing efficiency as high as 90%. Therefore, the above results confirm the effectiveness of the combined AC/DC potential mode in enhancing the microfluidic mixing efficiency within the T-shaped microchannel and the mixing performance of the case with the applied AC electric field with an intensity of 165 V/cm and a frequency of 4 Hz is the best among the cases.

The wavy pattern at the interface not only can enhance the mixing efficiency of the two streams, but the

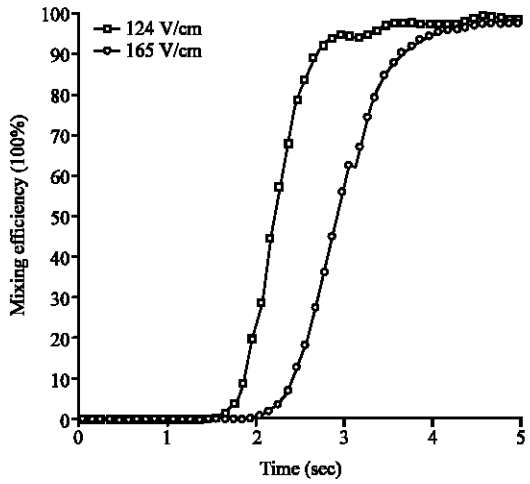

Fig. 6: Variation of mixing efficiency with time along the cross section at the outlet under application of AC electric field of amplitude 124, 165 and frequency 4 Hz at upper inlet and constant DC electric field intensity of 105 V/cm at lower inlet

position of the interface at the junction of the T-type microchannel can determine the relative amount of each fluid stream which enters the mixing channel. Therefore, the position of the interface governs the solution concentration in the fully-mixed state. In practice, the interface position is easily controlled by assigning a constant AC electric field intensity at the upper inlet and regulating the intensity of the DC electric field applied at the lower inlet. Note that the mean intensity of the AC electric field is 105 V/cm. When the DC electric field has an intensity of 132 V/cm, a significant difference exists in the intensities of the two electric fields (Fig. 7). The momentum of the stream introduced through the lower inlet (C = 1) is much greater than that of the stream introduced from the upper inlet (C = 0) and thus the interface between the two streams is located within the upper inlet channel. Consequently, the main mixing channel is filled almost entirely with fluid from the lower inlet and hence the fully-mixed dimensionless concentration has a value of 0.99. When the DC electric field intensity is reduced to 115 V/cm, the difference in the momentum of the two streams is reduced and thus the interface between the fluid streams is located just beneath the egress of the upper inlet into the junction region of the microchannel. Under these conditions, the bulk of the fluid entering the main mixing channel still originates from the lower inlet, but a greater amount of fluid from the upper inl*et al*so enters the mixing channel. As a result, the fully-mixed dimensionless concentration at the outlet reduces to 0.744. When the intensity of the DC electric field is further reduced to 105 V/cm, the momentums of the two streams are approximately equal and hence the fluid interface is located near the center of the junction region. As a result, the two streams flow into the microchannel in approximately equal proportions and thus the fully-mixed dimensionless concentration is 0.49. Finally, when the DC electric field intensity is reduced to 91 V/cm, the momentum of the stream entering from the upper inlet is greater than that of the stream entering from the lower inlet and thus the interface between them is located in the lower inlet. As a result, the mixing channel is filled almost entirely with fluid from the upper inlet and hence the fully-mixed dimensionless concentration has a value of 0.09 (Fig. 7a-d).

Note that in interpreting the x-axis, a negative (positive) value indicates that the applied DC field potential is lower (greater) than the mean value of the AC electric field potential (Fig. 8). As shown in Fig. 7, for a given AC electric field intensity, the value of the dimensionless concentration at the outlet of the microchannel is governed by the intensity of the DC electric field. Figure 8 shows that when the DC electric potential exceeds the mean value of the AC electric potential by 3 V or more, the mixing channel is filled with fluid from the lower inlet and the fully-mixed dimensionless concentration has a value close to one. However, when the DC electric potential is 2 V or more lower than the mean AC electric potential, the fluid from the upper inlet fills the main mixing channel and the value of the fully-mixed dimensionless concentration is close to zero. When the difference in the electric potentials applied at the two inlet channels falls within these two threshold values, i.e., -2 V~3 V, the fully-mixed concentration varies approximately linearly with the potential difference. Overall, the results presented in Fig. 8 confirm the ability of the combined AC/DC potential mode proposed in this study to achieve the proportional mixing of microfluidic elestro-osmotic flows.

As described earlier, the AC electric field applied at the upper inlet of the current T-shaped microchannel undergoes a process of half-wave rectification to prevent a backflow of the injected fluid into the reservoir (Fig. 9). For a sinusoidal electric field with an intensity of 165 V/cm and a frequency of 2 Hz, the amplitude remains at 165 V/cm following the rectification process, but the frequency increases to 4 Hz. The mean value of the rectified sinusoidal AC electric potential over the course of a single period is given by:

$$\bar{V} = \frac{2}{T}\int_0^{\frac{T}{2}} Amp\ \sin(\omega t)\ dt = \frac{2\times Amp}{\pi}$$

where, $\omega = 2\pi f$, in which f is the frequency, T is the period and Amp is the amplitude. From inspection, it is

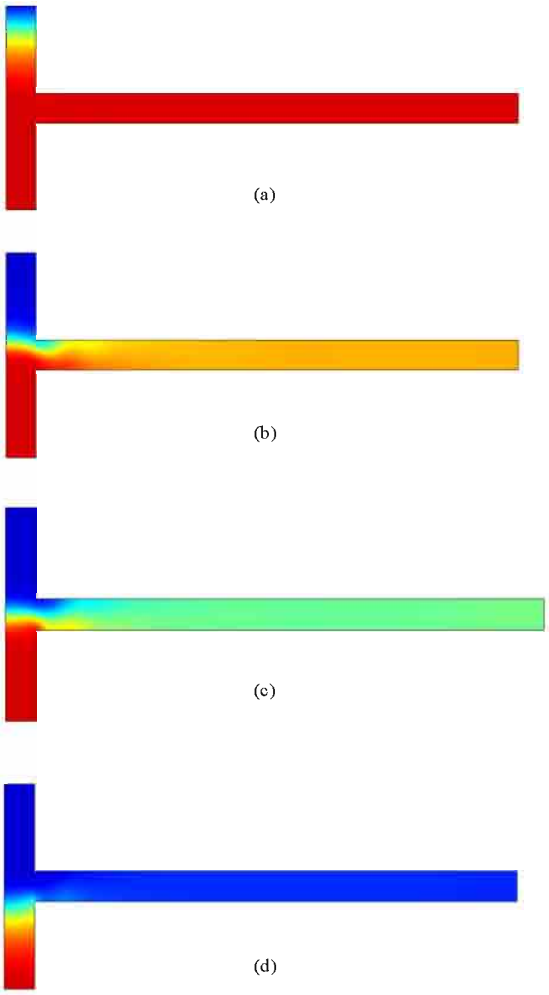

Fig. 7: Dimensionless concentration in fully-mixed condition under application of AC electric field of intensity 165 V/cm and frequency 4 Hz at upper inlet and constant DC electric field intensities of 132, 115, 105 and 91 V/cm at lower inlet. (a) DC voltage 132 V/cm, the dimensionless concentration at the outlet is 0.99. (b) DC voltage 115 V/cm, the dimensionless concentration at the outlet is 0.744. (c) DC voltage 105 V/cm, the dimensionless concentration at the outlet is 0.5 and (d) DC voltage 91 V/cm, the dimensionless concentration at the outlet is 0.09

apparent that the mean value of the AC electric field intensity is independent of the frequency. Since the relative proportion of the two species in the main mixing channel is determined by the difference between the DC and mean AC electric field intensities, the dimensionless concentration in the fully-mixed state is therefore also independent of the AC electric field frequency, as shown in Fig. 9.

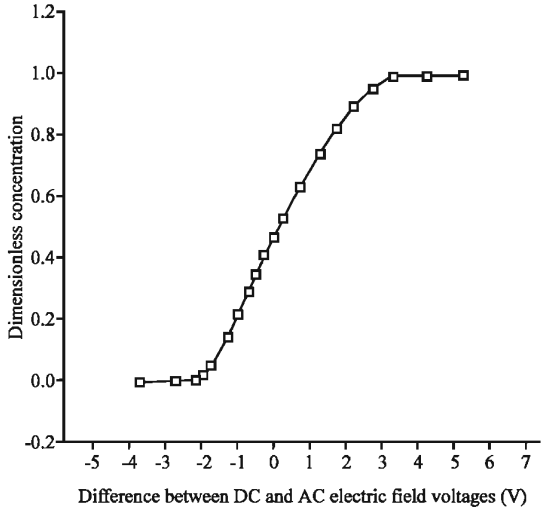

Fig. 8: Variation of dimensionless concentration in fully-mixed state with difference between DC and AC electric field voltages

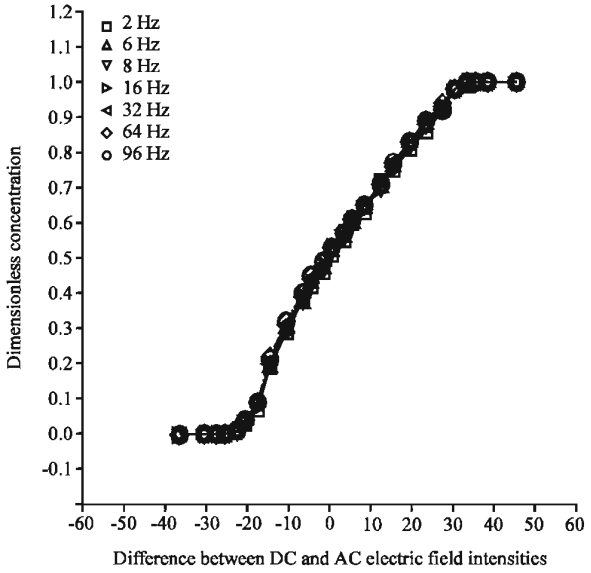

Fig. 9: Variation of fluid concentration in fully-mixed state with difference between DC and AC electric field intensities as function of AC frequency

Note that the maximum channel width is limited to 150 μm since this value represents the effective physical limit beyond which elestro-osmotic flow can not be induced. Note also that in deriving the results presented in the Fig. 10, the mixing channel was extended as required to ensure a fully-mixed condition as the channel width was progressively increased. From inspection, it is seen that the linear range bounded by the two threshold values of the DC electric field intensity expands slightly as the

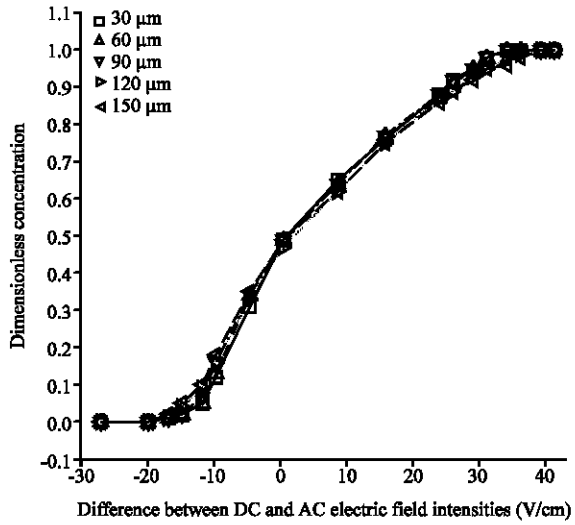

Fig. 10: Variation of fluid concentration in fully-mixed state with difference between DC and AC electric field intensities as function of mixing channel width

width of the microchannel is increased. However, the rate of change of the threshold values is significantly lower than that of the microchannel width, indicating that the threshold values are relatively insensitive to the microchannel width in the current range.

CONCLUSION

This study has proposed a T-shaped micromixer in which a half-wave rectified AC electric field is applied at the upper inlet, a DC electric field is applied at the lower inlet and the outlet is grounded. The combined effects of the DC and AC electric fields prompt the formation of a periodic waveform at the interface of the two fluid streams which increases the interfacial contact area and therefore improves the mixing efficiency. The numerical results have revealed that for a given AC electric field intensity, the position of the fluid interface within the intersection region of the microchannel can be regulated by adjusting the value of the DC electric potential. In this way, the relative amounts of the two fluid streams entering the mixing channel can be accurately controlled such that a proportional microfluidic mixing capability is obtained. For a constant AC electric potential, two threshold values of the DC electric field intensity have been found, corresponding to fully-mixed dimensionless concentrations of zero (upper inlet fluid only) and one (lower inlet fluid only), respectively. The results have shown that at DC electric field intensities between these two threshold values, the dimensionless concentration varies only as a function of the DC electric potential and is independent of the frequency of the AC electric field. Moreover, it has been shown that increasing the microchannel width has little effect on the fully-mixed values of the dimensionless concentration provided that the mixing length is adequately extended and results in no more than a minor expansion in the linear range bounded by the two threshold values.

ACKNOWLEDGMENTS

The current authors gratefully acknowledge the financial support provided to this study by the National Science Council of Taiwan under Grant No. NSC 95-2221-E-167-028 and NSC 95-2622-E-167-010-CC3.

REFERENCES

Ajdari, A., 1995. Electro-osmosis on inhomogeneously charged surfaces. Phys. Rev. Lett., 75 (4): 755-758.

Biddiss, E., D. Erickson and D. Li, 2004. Heterogeneous surface charge enhanced micromixing for electrokinetic flows. Anal. Chem., 76 (11): 3208-3213.

Branerbjerg, J., P. Gravesen, J.P. Krog and C.R. Nielsen, 1996. Experiments and simulations on a micro-mixer fabricated using a planar silicon/glass technology. Am. Soc. Mech. Eng. Dyn. Syst. Control Div. 59: 177-182.

Chang, C.C. and R.J. Yang, 2004. Computational analysis of electrokinetically-driven flow mixing in microchannels with patterned blocks. J. Micromech. Microeng., 14 (4): 550-558.

Chen, J.K., W.J. Luo and R.J. Yang, 2006. Elestro-osmotic flow driven by DC and AC electric fields in curved microchannels. Jap. J. Applied Phys., 45 (10A): 7983-7990.

Dutta, P. and A. Beskok, 2001. Analytical solution of time periodic elestro-osmotic flows: Analogies to stokes' second problem. Anal. Chem., 73 (21): 5097-5102.

Erickson, D. and D. Li, 2002. Influence of surface heterogeneity on electrokinetically driven microfluidic mixing. Langmuir, 18 (5): 1883-1892.

Hunter, R.J., 1986. Zeta Potential in Colloid Science Principles and Applications. Academic Press, London.

Lee, Y.K., J. Deval, P. Tabeling and C.M. Ho, 2001. Chaotic mixing in electrokinetically and pressure driven micro flows. In: Proceedings IEEE MEMS, pp: 483-486.

Lu, L.H., K.S. Ryu and C. Liu, 2002. A magnetic microstirrer and array for microfluidic mixing. J. MEMS., 11 (5): 462-469.

Luo, W.J., 2004a. Transient elestro-osmotic flow induced by DC or AC electric fields in a curved micro-tube. J. Colloid Interface Sci., 278 (2): 497-507.

Luo, W.J., 2004b. Flow bifurcations and transitions between Two rotating spheres. J. Mech., 20 (2): 95-105.

Luo, W.J., Y.J. Pan and R.J. Yang, 2005. Transient analysis of elestro-osmotic secondary flow induced by DC or AC electric field in a curved rectangular microchannel. J. Micromech. Microeng., 15 (3): 463-473.

Luo, W.J., 2006. Electrokinetically driven microfluidic mixing with patchwise surface heterogeneity and AC applied electric field. J. Colloid Interface Sci., 295 (2): 551-561.

Luo, W.J., K.F. Yarn and S.P. Hsu, 2007a. Analysis of electrokinetic mixing using AC electric field and patchwise surface heterogeneities. Jap. J. Applied Phys., 46 (4A): 1608-1616.

Luo, W.J., K.C. Chang, K.F. Yarn and M.H. Shih, 2007b. In Solid State Devices and Materials. Tsukuba International Congress Center, Tsukuba, Ibaraki, Japane.

Luo, W.J., K.F. Yarn, M.H. Shih and K.C. Yu, 2008. Microfluidic mixing utilizing electrokinetic instability stirred by electrical field intensity perturbations in a glass microchannel. Optoelect. Adv. Mater. Rapid Commun., 2 (2): 117-125.

Mengeaud, V., J. Josserand and H.H. Girault, 2002. Mixing processes in a zigzag microchannel: Finite element simulations and optical study. Anal. Chem., 74 (16): 4279-4286.

Miyake, R., T.S.J. Lammerink, M. Elwenspoek and J.H.J. Fluitman, 1993. Micro mixer with fast diffusion. Proceedings IEEE MEMS, pp: 248-253.

Oddy, M.H., J.G. Santiago and J.C. Mikkelsen, 2001. Electrokinetic instability micromixing. Anal. Chem., 73 (24): 5822-5832.

Qian, S. and H.H. Bau, 2002. A chaotic elestro-osmotic stirrer. Anal. Chem., 74 (15): 3616-3625.

Rife, J.C., M.I. Bell, J.S. Horwitz, M.N. Kabler, R.C.Y. Kabler, R.C.Y. Auyeung and W.J. Kim, 2000. Miniature valveless ultrasonic pumps and mixers, sens. Actuators. A, 86 (1-3): 135-140.

Voldman, J., M.L. Gray and M.A. Schmidt, 2000. Integrated liquid mixer/valve. J. MEMS., 9 (3): 295-302.

Yang, C. and D. Li, 1998. Analysis of electrokinetic effects on the liquid flow in rectangular microchannels. Colloids Surf. A, 143 (2-3): 339-353.

Yang, R.J. and W.J. Luo, 2002. Flow bifurcations between two rotating spheres. Theor. Comput. Fluid Dyn., 16 (2): 115-131.

Yang, R.J., C.H. Wu, T.I. Tseng and G.B. Lee, 2005. Enhancement of electrokinetically-driven flow mixing in microchannel with added side channels. Jap. J. Applied Phys., 44 (10): 7634-7642.